


Article

Poisoning Effects of Phosphorus, Potassium and Lead on V_2O_5 - WO_3 / TiO_2 Catalysts for Selective Catalytic Reduction with NH_3

Jifa Miao^{1,2,3}, Xianfang Yi^{1,2,3}, Qingfa Su^{1,2,3}, Huirong Li^{1,2,3}, Jinsheng Chen^{1,2,*}  and Jinxiu Wang^{1,2,*}

¹ Center for Excellence in Regional Atmospheric Environment, Institute of Urban Environment, Chinese Academy of Sciences, Xiamen 361021, China; jfmiao@iue.ac.cn (J.M.); xfyi@iue.ac.cn (X.Y.); qfsu@iue.ac.cn (Q.S.); hrli@iue.ac.cn (H.L.)

² Key Laboratory of Urban Environment and Health, Institute of Urban Environment, Chinese Academy of Sciences, Xiamen 361021, China

³ University of Chinese Academy of Sciences, Beijing 100049, China

* Correspondence: jschen@iue.ac.cn (J.C.); jxwang@iue.ac.cn (J.W.); Tel./Fax: +86-592-6190765 (J.C.); +86-592-6190548 (J.W.)

Received: 13 February 2020; Accepted: 17 March 2020; Published: 20 March 2020



Abstract: The poisoning effect of single elements on commercial V_2O_5 - WO_3 / TiO_2 catalysts has been studied in the past decades. In this study, the combined effects of two multi-element systems (phosphorus-potassium and phosphorus-lead) on V_2O_5 - WO_3 / TiO_2 catalysts were studied by diverse characterizations. The results show that potassium and lead can result in the deactivation of catalysts to different degrees by reacting with active acid sites and reducing the amount of V^{5+} . However, phosphorus displays slight negative influence on the NO_x conversion of the catalyst due to the comprehensive effect of reducing V^{5+} amount and generating new acid sites. The samples poisoned by phosphorus-potassium and phosphorus-lead have higher NO_x conversion than that by potassium or lead, because doped potassium or lead atoms may react with new acid sites generated by phosphate, which liberates more V-OH on the surface of catalysts and reduces the poisoning effects of potassium or lead on vanadium species and active oxygen species.

Keywords: commercial SCR catalysts; multi-element poisoning; phosphorus; lead; potassium; combined effect

1. Introduction

The selective catalytic reduction (SCR) of nitrogen oxides (NO_x) with ammonia is one of the most effective technologies to reduce NO_x emission generated by combustion process [1–3], such as coal-fired power plants and municipal solid waste incinerators [4]. The catalyst mostly used for this purpose is V_2O_5 - WO_3 / TiO_2 . V_2O_5 is considered as the active phase and WO_3 is considered as a promoter that inhibits the transformation of anatase to rutile, favors the spreading of the vanadia on the catalyst surface, and increases the acidity of the catalyst [5,6].

Though V_2O_5 - WO_3 / TiO_2 catalysts show excellent activity in NH_3 -SCR process, many compounds including alkali/alkali earth metal elements, Pb, Zn, P and As are found in exhaust flue gas streams, which can lead to the deactivation of SCR catalysts in their lifetime. The deactivation mechanism of single element was studied in the past decades [1,7–13]. Recently, the combined effects of different elements in the flue gas aroused the attention of scholars. Yu et al. [14,15] suggested that SO_2 in the flue gas promoted the activity of K- and Pb-poisoned catalysts. Kong et al. [16] discovered that new acid sites generated on the SCR catalyst by loading $HgCl_2$. Our recent work indicated SO_2 and HCl can

promote the activity of Pb-poisoned SCR catalyst [4]. However, few studies were about the combined effects of P and other poisoning elements. Schobing et al. [1] found the simultaneous presence of Ca and Zn on the catalyst increased the deactivation, but the additivity of individual effects was not observed and the presence of phosphates anions reduced the poisoning effects of Ca and Zn. Klimczak et al. [17] found an alleviated poisoning of Ca in the presence of phosphates and sulfates due to a regeneration of the ammonia adsorption capacity of the catalyst. It seems that phosphorus (P) could neutralize the negative effects of some poisoning elements, even though P has relatively small negative influence on V_2O_5 - WO_3 / TiO_2 catalysts in consideration of the large amount of phosphorus addition. However, Chen et al. [18] discovered that alkali metal had the strongest poisoning effect on the V-based catalyst, and the poisoning effect of Pb was between K_2O and Na_2O ($K_2O > PbO > Na_2O$). And K is a major component of alkali metals in the coal-fired flue gas. Tokarz et al. [19] measured a large amount of Pb contained in the flue gas of municipal solid waste incinerators. It is; therefore, desirable to study the combined poisoning effects of P and K or Pb on commercial V_2O_5 - WO_3 / TiO_2 catalysts.

In this work, the commercial V_2O_5 - WO_3 / TiO_2 catalyst was deactivated by P, K, Pb and the combination of P and K or Pb. The combined poisoning effects of P and K or Pb were studied by a series of characterizations. The influence of surface O, V, P and Ti species was investigated by X-ray photoelectron spectroscopy (XPS) and the amount and types of acid sites present in catalysts were further studied by temperature-programmed desorption of NH_3 (NH_3 -TPD) and in situ diffuse reflectance infrared Fourier-transform spectroscopy (in situ DRIFTS).

2. Results and Discussion

2.1. Catalytic Activity

Figure 1a shows the SCR activity of the catalyst samples in the temperature range of 250 to 380 °C under a GHSV of 60,000 h^{-1} . The experiments at each specific temperature were maintained for 1 h. The NO_x conversion of fresh sample keeps around 90% in the temperature range of 250 to 380 °C. Compared with fresh sample, the NO_x conversion of D-P (poisoned by P) decreases slightly (~4%). The poisoning effects of K and Pb on the V_2O_5 - WO_3 / TiO_2 catalyst obviously decrease the NO_x conversion of D-K (poisoned by K) and D-Pb (poisoned by Pb) sample. However, the NO_x conversion rates of D-P-K (poisoned by P and K) and D-P-Pb (poisoned by P and Pb) pretreated with $(NH_4)_2HPO_4$ are higher than that of D-K and D-Pb, respectively. It implies that the treatment with $(NH_4)_2HPO_4$ counteracts the poisoning effects of K and Pb on the catalyst to some degree. Furthermore, Figure S1a shows the N_2 selectivity of poisoned catalyst increases at increasing temperature in the range 250–280 °C. Then N_2 selectivity of poisoned catalyst decreases with increasing temperature above 300 °C.

Figure 1b shows the NO_x conversion of the fresh catalyst and poisoned samples at 350 °C for 3500 min. The fresh catalyst shows high stability. Its NO_x conversion reaches the stable stage in 10 min and keeps around 95% until the end of the test. The NO_x conversion rates of D-K and D-Pb samples also slightly decrease with time. The NO_x conversion rates of the catalysts treated by $(NH_4)_2HPO_4$ (D-P, D-P-K and D-P-Pb) decrease by 2%, 3% and 3%, respectively, in the first 1500 min, and then are relatively stable during the test. The N_2 selectivity of fresh sample keeps stable, and that of the poisoned catalyst decreases a little during the test (Figure S1b).

2.2. Structure and Surface Acid Sites

XRD patterns of fresh catalyst and poisoned samples are displayed in Figure 2. The $2\theta = 25.30^\circ$, 36.95° , 37.79° , 38.57° , 48.04° , 53.89° , 55.06° , 62.11° , 62.69° , 68.76° , 70.29° , 74.05° and 76.03° diffraction peaks correspond to tetragonal anatase phase of titanium dioxide (PDF card-03-065-5714). Only anatase phase TiO_2 is observed in all samples and it indicates that the dopants do not change the crystal type of TiO_2 . In addition, it also suggests the finely dispersed or amorphous V_2O_5 and other dopants on the

surface of TiO_2 . The SEM-EDS images of V and W evidence the presence of W, V and the dopants on the catalyst surface (Figure S2).

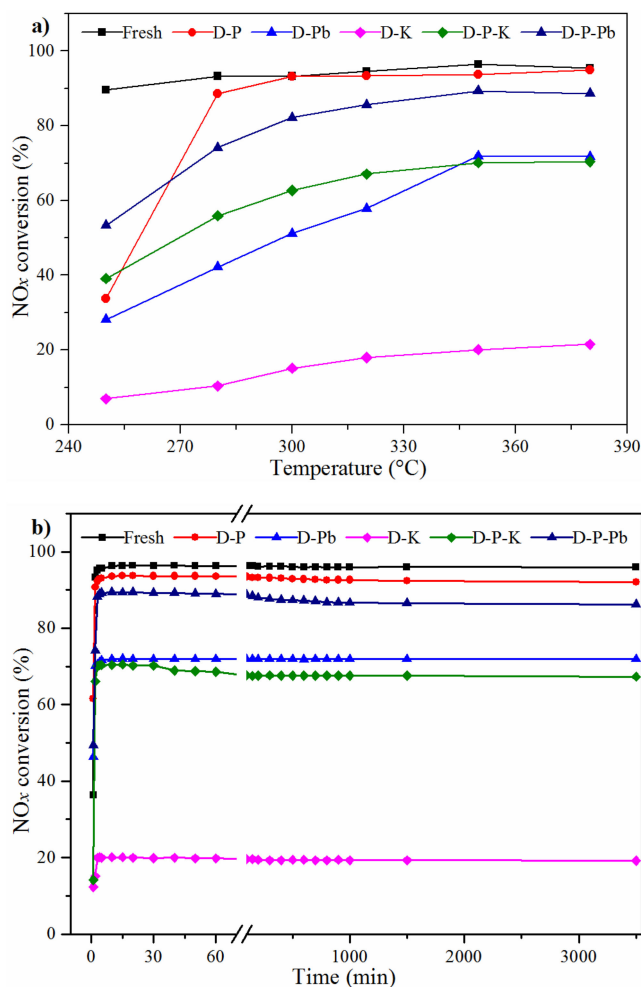


Figure 1. (a) NO_x conversion of fresh catalyst and poisoned catalyst. (b) NO_x conversion of fresh catalyst and poisoned catalyst at 350 °C with time. Reaction conditions: [NO] = [NH₃] = 500 ppm, [O₂] = 5 vol. %, total flow rate = 1.2 L/min, GHSV = 60,000 h⁻¹.

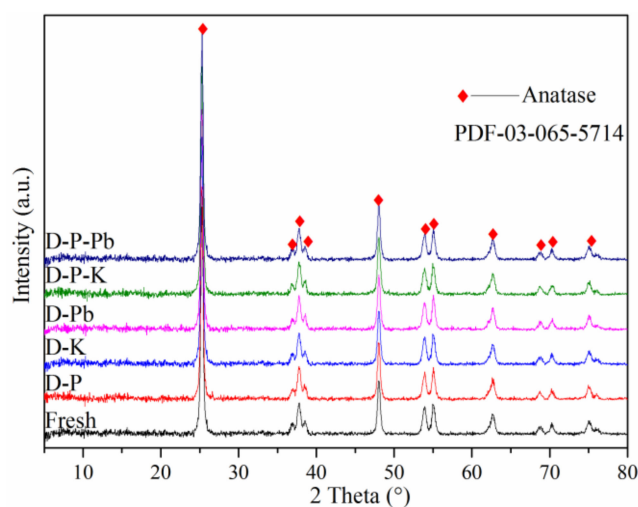


Figure 2. XRD patterns of fresh and poisoned catalysts.

Table 1 summarizes the element loading amount, specific surface areas (S_{BET}), total pore volume (V_{p}) and average pore diameter (D_{A}) for all catalysts. The N_2 adsorption-desorption isotherms of all samples and pore size distribution are displayed in Figures S3 and S4. According to the International Union of Pure and Applied Chemistry (IUPAC) classification, the isotherms are type-IV nitrogen isotherm corresponding to typical mesoporous materials. The S_{BET} and V_{p} of the D-Pb and D-K samples are almost similar to the fresh catalyst, suggesting that Pb and K have little influence on the pore structure of the catalyst. The treatment with $(\text{NH}_4)_2\text{HPO}_4$ decreases the S_{BET} and increases the D_{A} of the samples, The SEM images of fresh catalysts and poisoned samples are exhibited in Figure S5. A little agglomeration is observed on the samples containing P, which may block the pores and change S_{BET} and V_{p} of the samples.

Table 1. Element loading amount, specific surface areas, total pore volume and average pore diameter of samples.

Sample	Loading Amount (wt %)			S_{BET} (m^2/g)	V_{p}^* (cm^3/g)	D_{A} (nm)
	P	K	Pb			
Fresh	-	-	-	41.8	0.231	11.06
D-P	0.95	-	-	34.3	0.207	12.09
D-Pb	-	-	0.86	41.6	0.227	10.74
D-K	-	0.48	-	41.5	0.234	12.75
D-P-K	0.91	0.45	-	31.3	0.225	14.38
D-P-Pb	0.88	-	0.87	34.9	0.215	12.34

* V_{p} is obtained at the relative pressure of $P/P_0 = 0.99$; - denotes it is not detected by SEM-EDS.

The results of structure analysis imply that significant deactivation effect of Pb and K may well result from the chemical reaction between poisoning elements and active sites over catalysts. Moreover, the NO_x conversion of samples containing P and another poisoning element is not affected by the reduced S_{BET} . There may be other reasons for the activity change of these samples. Therefore, further characterizations were conducted.

It has been recognized that the surface acid sites over $\text{V}_2\text{O}_5\text{-WO}_3/\text{TiO}_2$ catalyst play a crucial role in the selective catalytic reduction process [4,20]. Therefore, the NH_3 -TPD was performed to investigate the combined effects of poison elements on acid sites of the catalyst. The NH_3 -TPD profile are exhibited in Figure 3. It shows that all curves recorded from 100–600 °C are divided into two parts. The part below 280 °C is attributed to NH_3 desorption on the weak acid sites, and the other part above 280 °C is ascribed to NH_3 desorption on the strong acid sites. The total amounts of NH_3 adsorption on each sample are calculated from the integrated areas of the corresponding curves and normalized by the value of Fresh sample. They are sequenced as follows: D-P (1.27) > fresh (1.00) > D-P-Pb (0.68) > D-Pb (0.64) > D-P-K (0.60) > D-K (0.23). It shows that the amount of desorbed NH_3 on the D-P sample increases by 27% compared with fresh sample especially the amount of NH_3 adsorbed on the weak acid sites. However, the Mass Spectrum (MS) signal of desorbed NH_3 decreases obviously with doping K (by 77%) or Pb (by 36%), which suggests the doping of K or Pb reduces the acidity of catalyst significantly. The treatment with $(\text{NH}_4)_2\text{HPO}_4$ increases the amount of NH_3 adsorption of K and Pb poisoning samples by 161% and 6%, respectively. It may be the reason that D-P-K and D-P-Pb samples have higher DeNO_x efficiency than D-K and D-Pb samples.

Besides the surface concentration of acid sites, the types of acid sites are also important for the SCR catalysts [21]. Therefore, a set of in situ DRIFTS experiments was conducted to obtain a thorough understanding of the interaction between NH_3 and the surface acid sites.

The in situ DRIFTS results of samples exposed to 500 ppm NH_3 in N_2 at 350 and 200 °C for 30 min are displayed in Figure 4. Figure 4a shows that three bands at 1605, 1401 and 1238 cm^{-1} are detected in the Fresh catalyst at 350 °C. It is recognized that the bands located at 1605 and 1238 cm^{-1} are ascribed to NH_3 adsorbed on Lewis acid sites [21–24], and the band at 1401 cm^{-1} is associated with asymmetric

deformation modes of ammonium ions on Brønsted acid sites [25,26]. The observed bands at 1610, 1426, 1409 and 1659 cm^{-1} on D-P sample are stronger obviously than that on fresh sample at 350 °C. The band located at 1659, 1426 and 1409 cm^{-1} were proved to be NH_3 adsorbed on the Brønsted acid sites [23,27,28]. It implies that the treatment with $(\text{NH}_4)_2\text{HPO}_4$ generates new Brønsted and Lewis acid sites and improves the acidity of $\text{V}_2\text{O}_5\text{-WO}_3/\text{TiO}_2$ catalyst [29–31]. For the in situ DRIFTS spectrum of D-K and D-Pb, only very weak bands are detected. It indicates that K and Pb can result in huge damage to Lewis acid sites and Brønsted acid sites. However, when K or Pb is introduced to the sample pretreated with $(\text{NH}_4)_2\text{HPO}_4$, the bands attributed to NH_3 adsorbed on Lewis acid sites and Brønsted acid sites can be detected with enhanced intensity. It suggests the treatment with $(\text{NH}_4)_2\text{HPO}_4$ can weaken the poisoning effects of K and Pb on the $\text{V}_2\text{O}_5\text{-WO}_3/\text{TiO}_2$ catalyst.

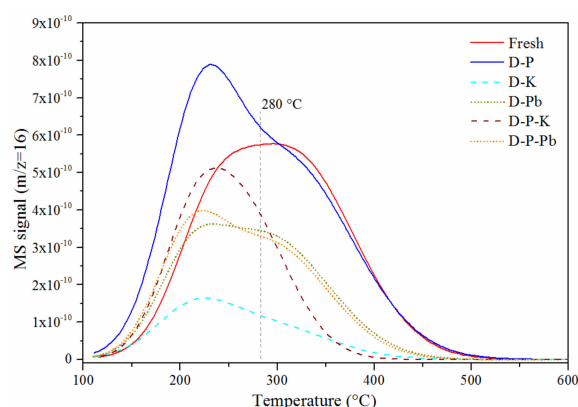


Figure 3. NH_3 -TPD profiles of fresh and poisoned catalyst samples.

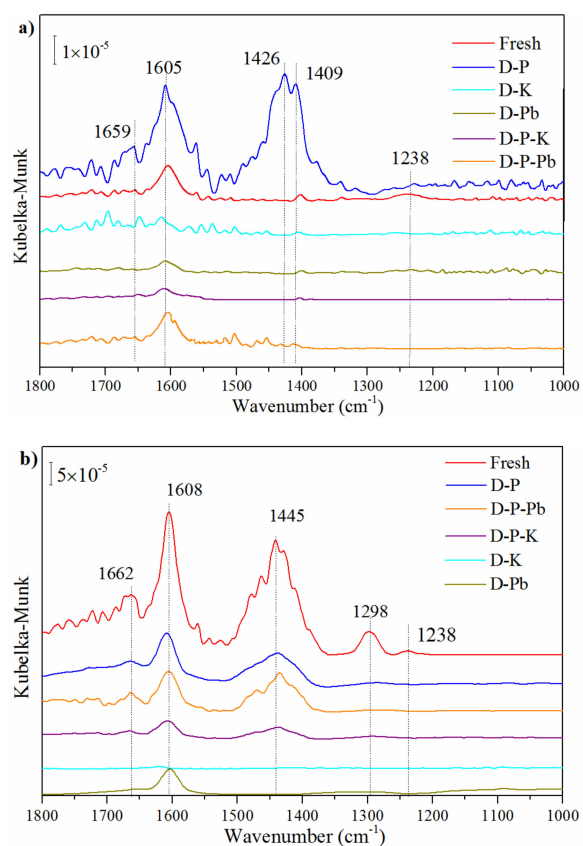


Figure 4. In situ DRIFTS spectra of NH_3 adsorption on fresh and poisoned catalysts at 350 °C (a) and 200 °C (b) for 30 min.

The stability of the adsorbed ammonia on the catalysts was analyzed by comparing the spectra of samples collected at 200 and 350 °C, respectively. The intensity of all peaks due to the adsorbed ammonia decreased with increasing temperature except the peaks detected on D-P. As shown in Figure 4b, the bands located at 1662, 1608, 1445, 1298 and 1238 cm^{-1} are observed on the fresh catalysts. The bands at 1662 and 1445 cm^{-1} are assigned to NH_4^+ chemisorbed on Brønsted acid site. The bands at 1608, 1298 and 1238 cm^{-1} are attributed to NH_3 adsorbed on the Lewis acid sites [21,32,33]. When the temperature reaches 350 °C, the bands on the fresh catalysts become to weaken and the band at 1298 cm^{-1} vanishes. However, the bands on the D-P samples still keep strong intensity especially the bands at 1426 and 1409 cm^{-1} . It implies that the acid sites generated by P species have higher thermo stability. This is maybe the reason the D-P has good NO_x conversion at high temperature. The Brønsted acid sites on the D-P-K and D-P-Pb decrease with increasing temperature clearly. The doped K and Pb atoms tend to react with acid sites generated by P species. The results suggest that the treatment with $(\text{NH}_4)_2\text{HPO}_4$ can weaken the poisoning effect of Pb and K on fresh catalyst because of the formation of new Lewis acid sites and Brønsted acid sites.

A total of 500 ppm NO and 5% O_2 were introduced to the D-P sample and fresh sample pretreated with NH_3 and purged with N_2 for 10 min. The reaction spectra between $\text{NO} + \text{O}_2$ and adsorbed NH_3 species are presented in Figure 5. For the spectrum of fresh catalyst, the band at 1238 cm^{-1} gradually weakens with time and vanishes after $\text{NO} + \text{O}_2$ is introduced for 30 min, and the bands at 1605 and 1401 cm^{-1} weaken during the test. In addition, new bands are detected at 1626 and 1599 cm^{-1} , which could be assigned to adsorbed NO_2 and bridged nitrate [34,35]. The results indicate that adsorbed NH_3 species on fresh sample are consumed in the $\text{NO} + \text{O}_2$ stream. For the spectrum of D-P sample, the bands at 1659, 1607, 1426 and 1409 cm^{-1} weaken during test time and the band at 1659 cm^{-1} almost vanishes for 30 min. A new band located at 1595 cm^{-1} assigned to adsorbed bridged nitrate is detected. The results indicate that adsorbed NH_3 species on Lewis acid sites and Brønsted acid sites, partly generated by the treatment of $(\text{NH}_4)_2\text{HPO}_4$, can be consumed in the $\text{NO} + \text{O}_2$ stream as well. The above experiments suggest that the reaction mechanism on the samples pretreated with $(\text{NH}_4)_2\text{HPO}_4$ still follows the Eley–Rideal mechanism: Adsorbed ammonia species react with gas-phase or weakly-adsorbed NO [36].

2.3. Surface Chemical State

XPS was carried out to illustrate the change of oxidation state of the active species after poisoning. Figure 6 shows the XPS results of O 1s, V 2p_{3/2}, P 2p and Ti 2p. The spectra of O 1s were fitted into three peaks which are the lattice oxygen in the metal oxides (O_γ), the surface oxygen by hydroxyl species (O_β) and the adsorbed oxygen or/and weakly bonded oxygen species (O_α) [21,37,38]. The positions and concentrations of oxygen species are displayed in the Table 2. Surface chemisorbed oxygen has been reported to be the most active oxygen and plays an important role in oxidation reactions [20,39]. It can be found that O_β concentration of D-P sample is higher than that of fresh sample, indicating that there are more hydroxyl species ($-\text{OH}$) after doping which can form $\text{P}-\text{OH}$ on the surface of catalysts [31]. However, the D-P sample has lower NO_x conversion than fresh catalyst, indicating $\text{P}-\text{OH}$ has lower activity than that of $\text{V}-\text{OH}$. The O_β concentration of D-K and D-Pb samples is lower than that of fresh sample, suggesting K and Pb can react with surface hydroxyl species and form $-\text{O}-\text{K}$ or $-\text{O}-\text{Pb}-\text{O}-$, in accordance with other researches [20,40]. For D-P-K and D-P-Pb samples, it can be found that O_β concentration increases largely, suggesting more $-\text{OH}$ species still exist on the catalyst surface. The binding energy value of O_γ shifts from 529.9 to 529.7 and 529.8 eV after the Pb and K doping. This may be because Pb and K donates electrons to lattice oxygen. However, in the D-P-K and D-P-Pb samples, the binding energy value of O_γ keeps similar to the fresh catalyst. It suggests that the treatment with $(\text{NH}_4)_2\text{HPO}_4$ may obstruct the electron interaction of Pb and K and the catalyst.

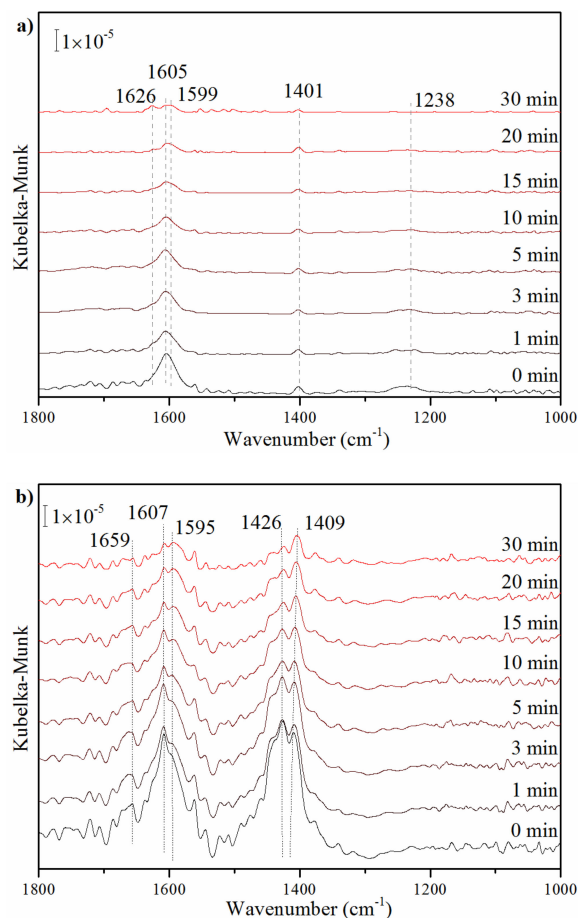


Figure 5. In situ DRIFTS spectra of the reaction between $\text{NO} + \text{O}_2$ and adsorbed NH_3 species over (a) fresh and (b) D-P at 350°C .

Table 2. The position and atom ratio of O spices in XPS spectra for each sample.

Samples	O_α %	O_β %	O_γ %
Fresh	532.4 (18.1)	531.3 (17.4)	529.9 (64.5)
D-P	532.3 (19.3)	531.2 (25.4)	529.9 (55.3)
D-Pb	532.3 (22.1)	531.0 (14.6)	529.7 (63.3)
D-K	532.3 (22.9)	531.0 (5.7)	529.8 (71.4)
D-P-Pb	532.4 (22.8)	531.4 (22.8)	529.9 (54.4)
D-P-K	532.3 (26.2)	531.3 (17.9)	530.0 (55.9)

Based on previous reports [41,42], the SCR activity of catalyst is positively correlated with the surface $\text{V}^{5+}/\text{V}^{4+}$ ratio. The spectra of $\text{V} 2p_{3/2}$ are fitted into two peaks related to V^{5+} (~ 517.1 eV) and V^{4+} (~ 516.2 eV) [43]. The atomic ratio of $\text{V}^{5+}/\text{V}^{4+}$ can be determined according to the peaks area ratio of $\text{V}^{5+}/\text{V}^{4+}$. Table 3 summarizes the peak position and atomic ratio of $\text{V}^{5+}/\text{V}^{4+}$ in different samples. The atomic ratio of $\text{V}^{5+}/\text{V}^{4+}$ decreases obviously after doping poisoning elements, indicating P, Pb and K can result in the transformation from V^{5+} into V^{4+} in $\text{V}_2\text{O}_5\text{-WO}_3/\text{TiO}_2$ catalysts. However, the adverse influence of P on surface $\text{V}^{5+}/\text{V}^{4+}$ ratio was much weaker than K and Pb. The atomic ratio of $\text{V}^{5+}/\text{V}^{4+}$ decreases from 1.21 to 0.43 and 0.51 after doping with K and Pb. Compared with D-K and D-Pb, the atomic ratio of $\text{V}^{5+}/\text{V}^{4+}$ in D-P-K and D-P-Pb samples increases largely. The result indicates that the treatment with $(\text{NH}_4)_2\text{HPO}_4$ can inhibit the transformation from V^{5+} into V^{4+} resulting from the adverse influence of Pb and K.

The P 2p binding energy of samples containing P is detected at 133.8 eV, suggesting that P in the samples exists in a pentavalent-oxidation state (P^{5+}) [44], and no peak is observed at 128.6 eV that is the characteristic binding energy of P 2p in Ti-P, indicating the absence of Ti-P bonds in the samples [29,30,45].

Table 3. XPS results of V 2p_{3/2} and surface atomic ratio of V⁵⁺/V⁴⁺ for each sample.

Samples	Binding Energy (eV)		V ⁵⁺ /V ⁴⁺
	V ⁴⁺	V ⁵⁺	
Fresh	516.1	517.1	1.21
D-P	516.2	517.1	0.86
D-Pb	516.1	517.1	0.51
D-K	516.2	517.1	0.43
D-P-K	516.2	517.1	0.71
D-P-Pb	516.3	517.2	0.83

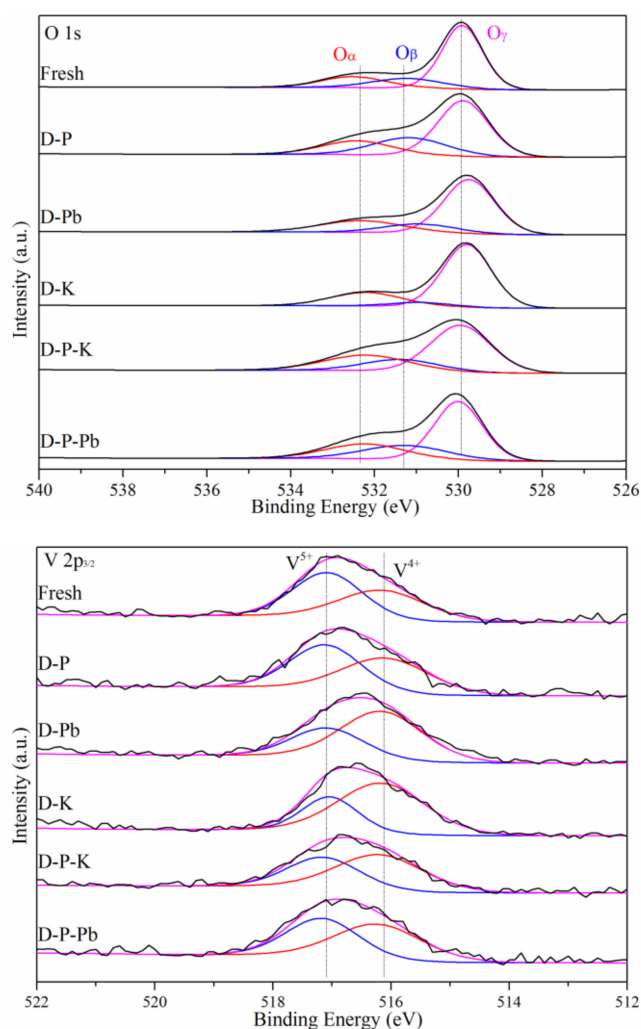


Figure 6. Cont.

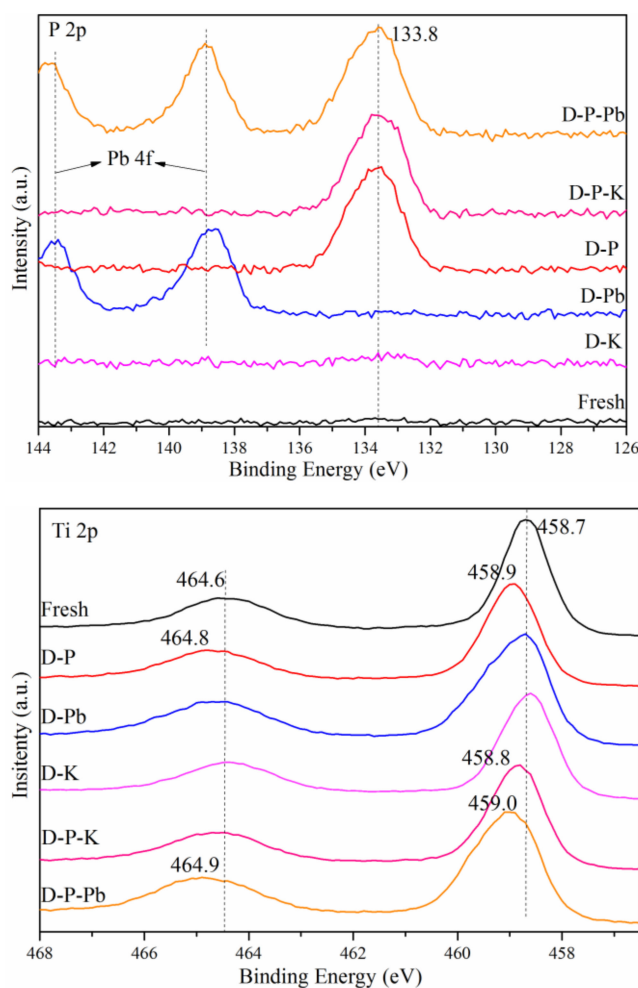


Figure 6. XPS spectra of the O 1s, V 2p_{3/2}, P 2p and Ti 2p of fresh and poisoned samples.

For the spectra of Ti 2p, two peaks centered at 458.6–459 eV and 464.4–464.9 eV can be ascribed to Ti 2p_{3/2} and Ti 2p_{1/2}, respectively, suggesting the presence of Ti⁴⁺ in all samples [25,46]. When the catalyst treated with (NH₄)₂HPO₄, the Ti 2p_{3/2} and Ti 2p_{1/2} peaks shift to higher energies, from 458.7 to 458.9 eV and 464.6 to 464.8 eV, respectively. It means the titanium species in D-P samples have lower density of electron cloud density than that in fresh samples [45,47]. It may be because the electrons around the titanium species transfer to oxygen species, which interact with P dopants. It also proves that P⁵⁺ can replace part of Ti⁴⁺ in TiO₂ lattice to form a Ti–O–P linkage. The similar location of the Ti 2p peaks for fresh, D-K and D-Pb samples, indicates that K and Pb may not react with TiO₂ [4,48]. In addition, D-P-K and D-P-Pb have a similar Ti 2p peak center with D-P, which implies that K or Pb does not affect the reaction between P species and TiO₂. The XPS spectra of W 4f were displayed in the Figure S6 and the information was supplied in the Supplementary Materials.

2.4. Poisoning Effect of Phosphorus, Potassium and Lead on V₂O₅-WO₃/TiO₂ Catalysts

Based on the NH₃-TPD, DRIFT, XPS spectra analysis and previous studies [29,49,50], the proposed combined poisoning effect of phosphorus, potassium or lead on V₂O₅-WO₃/TiO₂ can be concluded in Figure 7. For fresh catalyst, based on Eley–Rideal mechanism, the adsorbed NH₄⁺ species on –OH can be activated by V⁵⁺ active sites and react with NO in the flue gas [51,52]. The poisoning effects of K and Pb on the catalyst can be assigned to the neutralization of the acid sites, the decrease of surface chemisorption oxygen and the reduction of V⁵⁺ species [10,40]. This results in weakening the NH₃ adsorption capacity and reducibility of the catalyst. After the treatment with (NH₄)₂HPO₄, the doped P species occupy the acid sites. However, new Brønsted acid sites (P–OH) form [31], and the acid sites

also have the ability to adsorb NH_3 . The NH_4^+ species adsorbed on the Brønsted acid sites (P–OH) could be activated by surface V active sites due to the excellent redox property of nearby V^{5+} species. Hence, the slightly weakened NH_3 -SCR performance of D-P samples can be assigned to the reduction of V^{5+} species. For D-P-K and D-P-Pb, the in situ DRIFTS analysis results suggest doped Pb and K atoms may react with acid sites generated by phosphate, and make them inactive in the adsorption of NH_3 . Each K atom consumes one acid site, and each Pb atom reacts with two acid sites. Hence, it seems that more K and Pb around the P atom will liberate more V–OH on the surface of catalysts, so the treatment with $(\text{NH}_4)_2\text{HPO}_4$ alleviates the poisoning effect of potassium or lead on the catalysts [53].

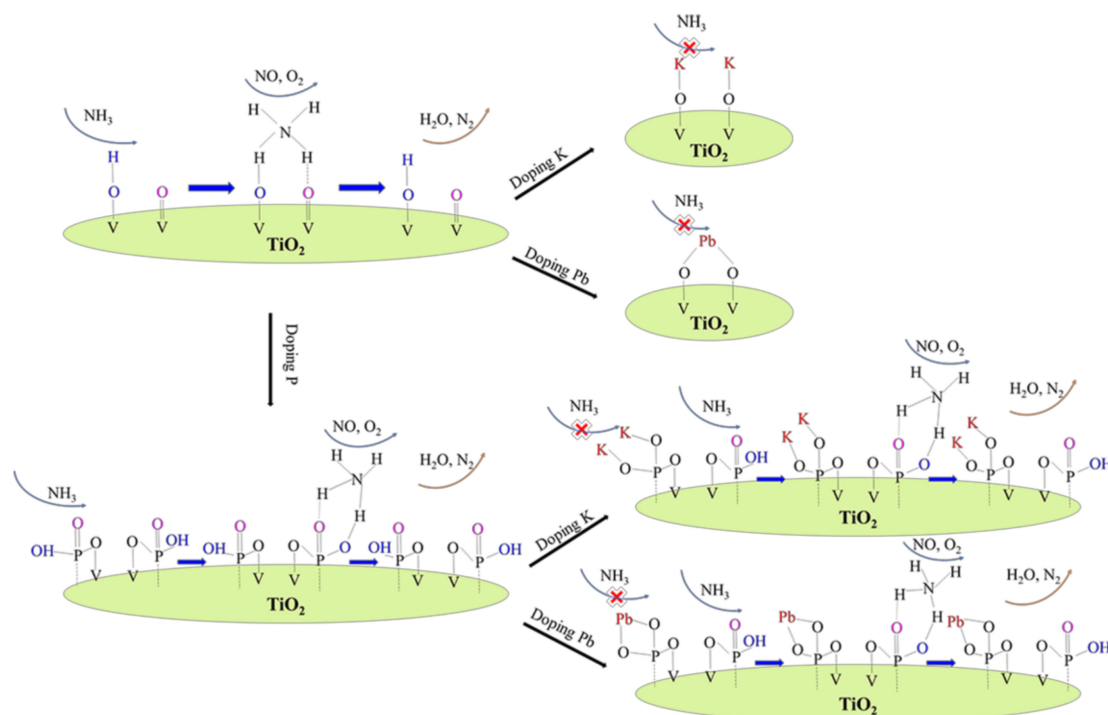


Figure 7. Schematic diagram of the combined effect of phosphorus, potassium and or lead on $\text{V}_2\text{O}_5\text{-WO}_3/\text{TiO}_2$.

3. Materials and Methods

3.1. Catalysts Preparation

The commercial $\text{V}_2\text{O}_5\text{-WO}_3/\text{TiO}_2$ catalyst (named as Fresh, with 1.16 wt.% V and 2.42 wt.% W) was ground and sieved to 60–80 mesh. All the chemicals used in the catalyst preparation process were analytical grade and purchased from Sinopharm Chemical Reagent Co., Ltd (Shanghai, China). The P poisoned samples were prepared by impregnating the commercial catalyst particles into aqueous $(\text{NH}_4)_2\text{HPO}_4$ (0.25 mol/L) solution for 6 h at room temperature. Then the samples were dried at 105 °C for 12 h followed by calcination at 500 °C for 4 h in a muffle furnace. The P poisoned catalyst was denoted as D-P. Fresh catalysts and D-P sample were impregnated into aqueous KNO_3 (0.13 mol/L) or $\text{Pb}(\text{NO}_3)_2$ (0.25 mol/L) solution for 6 h at room temperature. Then the samples were dried at 105 °C for 12 h followed by calcination at 500 °C for 4 h in a muffle furnace. The samples were denoted as D-K, D-Pb, D-P-K and D-P-Pb. The element loading amount detected by SEM-EDS is summarized in Table 1.

3.2. Activity Test

The catalytic activities of the samples were evaluated in a simulated fixed-bed reactor made of quartz tube with the dimensions of $\Phi 6.2 \times 580$ mm in the laboratory. The simulated flue gas consisted of 500 ppm NO, 500 ppm NH_3 , 5% O_2 and N_2 balance. In each experimental run, the catalysts loaded

in the reactor were 1.2 cm³ and the gas hourly space velocity (GHSV) was kept at 60,000 h⁻¹. For this system, the concentrations of NO, NO₂ and NH₃ were measured by an Antaris IGS analyzer (Thermo Fisher Company, Waltham, M.A., USA) and the concentration of O₂ was measured by a flue gas analyzer (T-350, Testo Company, Hampshire, United Kingdom).

The conversion of NO_x was defined as:

$$\text{NOx conversion} = \frac{C_{\text{NO}_x,\text{in}} - C_{\text{NO}_x,\text{out}}}{C_{\text{NO}_x,\text{in}}} \times 100\%$$

$$\text{N}_2 \text{ selectivity} = 1 - \frac{2C_{\text{N}_2\text{O},\text{out}}}{C_{\text{NO}_x,\text{in}} + C_{\text{NH}_3,\text{in}} - C_{\text{NO}_x,\text{out}} - C_{\text{NH}_3,\text{out}}} \times 100\%$$

where $C_{\text{NO}_x,\text{in}}$ and $C_{\text{NO}_x,\text{out}}$ are the NO_x concentration (NO + NO₂) of the simulated gas stream in the inlet and outlet of the reactor, $C_{\text{NH}_3,\text{in}}$ and $C_{\text{NH}_3,\text{out}}$ are the inlet and outlet concentrations of NH₃, and $C_{\text{N}_2\text{O},\text{out}}$ is the outlet concentration of N₂O.

3.3. Catalysts Characterization

The morphology and elemental analysis of samples was conducted by scanning electron microscope-energy dispersive X-ray spectrometer (SEM-EDS, S-4800, Hitachi, Tokyo, and 51-ADD0009, Horiba, Tokyo; Japan) and X-ray fluorescence spectrometer (XRF, Axios mAX, PANalytical B.V., Almelo, Netherlands) equipped with a Rh-anode X-ray tube. The Brunauer–Emmett–Teller (BET) specific surface area and porosities of the samples were measured on a NOVA 1200e surface area and pore size analyzer (Quantachrome, Boynton Beach, F.L., USA) at 77 K. X-ray diffraction (XRD) patterns were recorded on X Pert Pro XRD diffractometer (PANalytical B.V., Almelo, Netherlands) with Cu K α radiation (40 kV, 40 mA).

The temperature-programmed desorption of ammonia (NH₃-TPD) on samples was carried out on a chemisorption analyzer (ChemBET-3000TPR-TPD, Quantachrome, Boynton Beach, F.L., USA)-mass spectrum (DYCOR LC-D200, Ametek, Kent, O.H., USA). A total of 100 mg of the sample was treated in helium at 500 °C for 1 h and cooled to room temperature. Then the sample was exposed to 5% NH₃ for 40 min and subsequently purged with helium at 100 °C for 30 min to remove weakly-adsorbed NH₃ from the surface. Finally, the sample was heated to 600 °C at a rate of 10 °C/min in He and the signal of NH₃ was recorded by mass spectrum.

In situ diffuse reflectance infrared Fourier-transform spectra (DRIFTS) were collected using a Bruker Vertex 70 infrared spectrometer (Billerica, M.A., USA) with KBr optics and a mercury-cadmium-telluride (MCT) detector. The sample was treated at 500 °C for 1 h and then cooled to the desired temperature in N₂ atmosphere. The spectra were collected with 500 ppm NH₃ in N₂ at the set time. All the spectra were collected at a resolution of 4 cm⁻¹ by accumulating 64 scans. The spectra obtained in this study were transformed into absorption spectra by using Kubelka–Munk function.

X-ray photoelectron spectra (XPS) were measured with a Thermo ESCALAB 250 (Waltham, M.A., USA) using monochromated Al K α X-rays ($h\nu = 1486.6$ eV) as a radiation source at 150 W. Sample charging effects were eliminated by correcting the observed spectra with the C 1s binding energy (BE) value of 284.6 eV. The analysis of XPS spectra of samples was conducted by “Avantage” software supplied by Thermo Fisher Scientific Corporation, and uses “Scofield factor” as sensitive factor.

4. Conclusions

In this study, P, K and Pb decrease the DeNO_x efficiency of commercial V₂O₅-WO₃/TiO₂ catalysts to different degrees. Furthermore, the doping of P, K and Pb does not change crystalline phase and textural structure of commercial catalysts. However, the treatment with (NH₄)₂HPO₄ improves the NO_x conversion of Pb- and K-poisoned catalysts. That may be because the samples pretreated with (NH₄)₂HPO₄ have higher content of acid sites with higher thermal stability. Moreover, they have increased V⁵⁺/V⁴⁺ ratio and active oxygen species, including V-OH and P-OH, on the surface of

catalysts. It is believed that the treatment with $(\text{NH}_4)_2\text{HPO}_4$ can decrease the poisoning effects of K and Pb on commercial $\text{V}_2\text{O}_5\text{-WO}_3/\text{TiO}_2$ catalysts. This work may offer the reference to further research in the complex poisoning effects of multiple elements on commercial $\text{V}_2\text{O}_5\text{-WO}_3/\text{TiO}_2$ catalysts.

Supplementary Materials: The following are available online at <http://www.mdpi.com/2073-4344/10/3/345/s1>, Figure S1: (a) The N_2 selectivity of fresh and poisoned samples; (b) the N_2 selectivity of fresh and poisoned samples at 350 °C with time, Figure S2: The SEM-EDS images of fresh and poisoned catalyst, Figure S3: N_2 adsorption-desorption isotherm of fresh and poisoned samples, Figure S4: The pore size distribution of fresh and poisoned samples, Figure S5: The SEM images of fresh catalysts and poisoned samples, Figure S6: XPS spectra of the W 4f of fresh and poisoned samples.

Author Contributions: Conceptualization, J.M., J.W. and J.C.; Data curation, J.W.; Investigation, J.M., X.Y. and Q.S.; Supervision, J.C. and J.W.; Writing—original draft, J.M.; Writing—review and editing, J.C. and J.W. All authors have read and agree to the published version of the manuscript.

Funding: This work is financially supported by Youth Innovation Promotion Association, Chinese Academy of Sciences (2020309), the Strategic Priority Research Program of the Chinese Academy of Sciences (XDB05050500), Bureau of Science and Technology, Fujian Province, China (2015H0043) and Fujian Institute of Innovation, Chinese Academy of Sciences.

Acknowledgments: The authors are grateful to the tests offered by the Analysis and Testing Center, Institute of Urban Environment, Chinese Academy of Sciences, Xiamen.

Conflicts of Interest: The authors declare no conflicts of interest.

References

- Schobing, J.; Tschamber, V.; Brillhac, J.F.; Auclair, A.; Vonarb, R. Investigation of the impact of calcium, zinc and phosphorus on DeNO_x activity of a commercial SCR catalyst. *Top. Catal.* **2016**, *59*, 1013–1019. [[CrossRef](#)]
- Peng, Y.; Li, J.; Si, W.; Luo, J.; Wang, Y.; Fu, J.; Li, X.; Crittenden, J.; Hao, J. Deactivation and regeneration of a commercial SCR catalyst: Comparison with alkali metals and arsenic. *Appl. Catal. B Environ.* **2015**, *168*, 195–202. [[CrossRef](#)]
- Putluru, S.S.R.; Schill, L.; Gardini, D.; Mossin, S.; Wagner, J.B.; Jensen, A.D.; Fehrmann, R. Superior DeNO_x activity of $\text{V}_2\text{O}_5\text{-WO}_3/\text{TiO}_2$ catalysts prepared by deposition–precipitation method. *J. Mater. Sci.* **2014**, *49*, 2705–2713. [[CrossRef](#)]
- Miao, J.; Li, H.; Su, Q.; Yu, Y.; Chen, Y.; Chen, J.; Wang, J. The combined promotive effect of SO_2 and HCl on Pb-poisoned commercial $\text{NH}_3\text{-SCR}$ $\text{V}_2\text{O}_5\text{-WO}_3/\text{TiO}_2$ catalysts. *Catal. Commun.* **2019**, *125*, 118–122. [[CrossRef](#)]
- Nicosia, D.; Elsener, M.; Kröcher, O.; Jansohn, P. Basic investigation of the chemical deactivation of $\text{V}_2\text{O}_5/\text{WO}_3\text{-TiO}_2$ SCR catalysts by potassium, calcium, and phosphate. *Top. Catal.* **2007**, *42*, 333–336. [[CrossRef](#)]
- Madia, G.; Elsener, M.; Koebel, M.; Raimondi, F.; Wokaun, A. Thermal stability of vanadia-tungsta-titania catalysts in the SCR process. *Appl. Catal. B Environ.* **2002**, *39*, 181–190. [[CrossRef](#)]
- Kling, Å.; Andersson, C.; Myringer, Å.; Eskilsson, D.; Järås, S.G. Alkali deactivation of high-dust SCR catalysts used for NO_x reduction exposed to flue gas from 100 MW-scale biofuel and peat fired boilers: Influence of flue gas composition. *Appl. Catal. B Environ.* **2007**, *69*, 240–251. [[CrossRef](#)]
- Khodayari, R.; Odenbrand, C.U.I. Deactivating effects of lead on the selective catalytic reduction of nitric oxide with ammonia over a $\text{V}_2\text{O}_5/\text{WO}_3/\text{TiO}_2$ catalyst for waste incineration applications. *Ind. Eng. Chem. Res.* **1998**, *37*, 1196–1202. [[CrossRef](#)]
- Hu, W.; Gao, X.; Deng, Y.; Qu, R.; Zheng, C.; Zhu, X.; Cen, K. Deactivation mechanism of arsenic and resistance effect of SO_4^{2-} on commercial catalysts for selective catalytic reduction of NO_x with NH_3 . *Chem. Eng. J.* **2016**, *293*, 118–128. [[CrossRef](#)]
- Chen, J.P.; Yang, R.T. Mechanism of poisoning of the $\text{V}_2\text{O}_5/\text{TiO}_2$ catalyst for the reduction of NO by NH_3 . *J. Catal.* **1990**, *125*, 411–420. [[CrossRef](#)]
- Hiroiyuki, K.; Katsumi, T.; Odenbrand, C.U.I. The role of K_2O in the selective reduction of NO with NH_3 over a $\text{V}_2\text{O}_5(\text{WO}_3)\text{-TiO}_2$ commercial selective catalytic reduction catalyst. *J. Mol. Catal. A Chem.* **1999**, *139*, 189–198.
- Larsson, A.C.; Einvall, J.; Sanati, M. Deactivation of SCR catalysts by exposure to aerosol particles of potassium and zinc salts. *Aerosol Sci. Technol.* **2007**, *41*, 369–379. [[CrossRef](#)]

13. Odenbrand, C.U.I. CaSO₄ deactivated V₂O₅-WO₃/TiO₂ SCR catalyst for a diesel power plant. Characterization and simulation of the kinetics of the SCR reactions. *Appl. Catal. B Environ.* **2018**, *234*, 365–377. [[CrossRef](#)]
14. Yu, Y.; Wang, J.; Chen, J.; Meng, X.; Chen, Y.; Chi, H. Promotive effect of SO₂ on the activity of a deactivated commercial selective catalytic reduction catalyst: An *in situ* DRIFT study. *Ind. Eng. Chem. Res.* **2014**, *53*, 16229–16234. [[CrossRef](#)]
15. Yu, Y.; Miao, J.; He, C.; Chen, J.; Li, C.; Douthwaite, M. The remarkable promotional effect of SO₂ on Pb-poisoned V₂O₅-WO₃/TiO₂ catalysts: An in-depth experimental and theoretical study. *Chem. Eng. J.* **2018**, *338*, 191–201. [[CrossRef](#)]
16. Kong, M.; Liu, Q.; Jiang, L.; Guo, F.; Ren, S.; Yao, L.; Yang, J. Property influence and poisoning mechanism of HgCl₂ on V₂O₅-WO₃/TiO₂ SCR-DeNO_x catalysts. *Catal. Commun.* **2016**, *85*, 34–38. [[CrossRef](#)]
17. Klimczak, M.; Kern, P.; Heinzelmann, T.; Lucas, M.; Claus, P. High-throughput study of the effects of inorganic additives and poisons on NH₃-SCR catalysts—Part I: V₂O₅-WO₃/TiO₂ catalysts. *Appl. Catal. B Environ.* **2010**, *95*, 39–47. [[CrossRef](#)]
18. Chen, J.P.; Buzanowski, M.A.; Yang, R.T.; Cichanowicz, J.E. Deactivation of the vanadia catalyst in the selective catalytic reduction process. *J. Air Waste Manage. Assoc.* **1990**, *40*, 1403–1409. [[CrossRef](#)]
19. Tokarz, M.; Järårs, S.; Persson, B. Poisoning of De-NO_x SCR catalyst by flue gases from a waste incineration plant. *Stud. Surf. Sci. Catal.* **1991**, *68*, 523–530.
20. Chen, L.; Li, J.; Ge, M. The poisoning effect of alkali metals doping over nano V₂O₅-WO₃/TiO₂ catalysts on selective catalytic reduction of NO_x by NH₃. *Chem. Eng. J.* **2011**, *170*, 531–537. [[CrossRef](#)]
21. Song, L.; Zhang, R.; Zang, S.; He, H.; Su, Y.; Qiu, W.; Sun, X. Activity of selective catalytic reduction of NO over V₂O₅/TiO₂ catalysts preferentially exposed anatase [18] and [10] facets. *Catal. Lett.* **2017**, *147*, 934–945. [[CrossRef](#)]
22. Yu, W.; Wu, X.; Si, Z.; Weng, D. Influences of impregnation procedure on the SCR activity and alkali resistance of V₂O₅-WO₃/TiO₂ catalyst. *Appl. Surf. Sci.* **2013**, *283*, 209–214. [[CrossRef](#)]
23. Wang, S.; Guo, R.; Pan, W.; Li, M.; Sun, P.; Liu, S.; Liu, S.; Sun, X.; Liu, J. The deactivation mechanism of Pb on the Ce/TiO₂ catalyst for the selective catalytic reduction of NO_x with NH₃: TPD and DRIFT studies. *Phys. Chem. Chem. Phys.* **2017**, *19*, 5333–5342. [[CrossRef](#)] [[PubMed](#)]
24. Cao, J.; Yao, X.; Yang, F.; Chen, L.; Fu, M.; Tang, C.; Dong, L. Improving the denitration performance and K-poisoning resistance of the V₂O₅-WO₃/TiO₂ catalyst by Ce⁴⁺ and Zr⁴⁺ co-doping. *Chin. J. Catal.* **2019**, *40*, 95–104. [[CrossRef](#)]
25. Zhang, S.; Zhong, Q. Surface characterization studies on the interaction of V₂O₅-WO₃/TiO₂ catalyst for low temperature SCR of NO with NH₃. *J. Solid State Chem.* **2015**, *221*, 49–56. [[CrossRef](#)]
26. Shi, Y.; Shu, H.; Zhang, Y.; Fan, H.; Zhang, Y.; Yang, L. Formation and decomposition of NH₄HSO₄ during selective catalytic reduction of NO with NH₃ over V₂O₅-WO₃/TiO₂ catalysts. *Fuel Process. Technol.* **2016**, *150*, 141–147. [[CrossRef](#)]
27. Peng, Y.; Si, W.; Li, X.; Chen, J.; Li, J.; Crittenden, J.; Hao, J. Investigation of the poisoning mechanism of lead on the CeO₂-WO₃ catalyst for the NH₃-SCR reaction via *in situ* IR and Raman spectroscopy measurement. *Environ. Sci. Technol.* **2016**, *50*, 9576–9582. [[CrossRef](#)]
28. Gan, L.; Chen, J.; Peng, Y.; Yu, J.; Tran, T.; Li, K.; Wang, D.; Xu, G.; Li, J. NO_x removal over V₂O₅/WO₃-TiO₂ prepared by a grinding method: Influence of the precursor on vanadium dispersion. *Ind. Eng. Chem. Res.* **2017**, *57*, 150–157. [[CrossRef](#)]
29. Li, X.; Li, K.; Peng, Y.; Li, X.; Zhang, Y.; Wang, D.; Chen, J.; Li, J. Interaction of phosphorus with a FeTiO_x catalyst for selective catalytic reduction of NO_x with NH₃: Influence on surface acidity and SCR mechanism. *Chem. Eng. J.* **2018**, *347*, 173–183. [[CrossRef](#)]
30. Shao, G.; Wang, F.; Ren, T.; Liu, Y.; Yuan, Z. Hierarchical mesoporous phosphorus and nitrogen doped titania materials: Synthesis, characterization and visible-light photocatalytic activity. *Appl. Catal. B Environ.* **2009**, *92*, 61–67. [[CrossRef](#)]
31. Hiroyuki, K.; Katsumi, T.; Odenbrand, C.U.I. Surface acid property and its relation to SCR activity of phosphorus added to commercial V₂O₅(WO₃)/TiO₂ catalyst. *Catal. Lett.* **1998**, *53*, 65–71.
32. Dong, Y.; Qu, R.; Hao, S.; Zheng, C.; Cen, K. Investigation of the promotion effect of WO₃ on the decomposition and reactivity of NH₄HSO₄ with NO on V₂O₅-WO₃/TiO₂ SCR catalysts. *RSC Adv.* **2016**, *6*, 55584–55592.
33. Parvulescu, V.I.; Boghosian, S.; Parvulescu, V.; Jung, S.M.; Grange, P. Selective catalytic reduction of NO with NH₃ over mesoporous V₂O₅-TiO₂-SiO₂ catalysts. *J. Catal.* **2003**, *217*, 172–185. [[CrossRef](#)]

34. Chen, L.; Li, J.; Ge, M. Promotional effect of Ce-doped V₂O₅-WO₃/TiO₂ with low vanadium loadings for selective catalytic reduction of NO_x by NH₃. *J. Phys. Chem. C* **2009**, *113*, 21177–21184. [[CrossRef](#)]
35. Jiang, B.Q.; Wu, Z.B.; Liu, Y.; Lee, S.C.; Ho, W.K. DRIFT study of the SO₂ effect on low-temperature SCR reaction over Fe-Mn/TiO₂. *J. Phys. Chem. C* **2010**, *114*, 4961–4965. [[CrossRef](#)]
36. Nova, I.; Lietti, L.; Tronconi, E.; Forzatti, P. Dynamics of SCR reaction over a TiO₂-supported vanadia-tungsta commercial catalyst. *Catal. Today* **2000**, *60*, 73–82. [[CrossRef](#)]
37. Guo, R.; Wang, Q.; Pan, W.; Chen, Q.; Ding, H.; Yin, X.; Yang, N.; Lu, C.; Wang, S.; Yuan, Y. The poisoning effect of heavy metals doping on Mn/TiO₂ catalyst for selective catalytic reduction of NO with NH₃. *J. Mol. Catal. A Chem.* **2015**, *407*, 1–7. [[CrossRef](#)]
38. Chang, H.Z.; Shi, C.N.; Li, M.G.; Zhang, T.; Wang, C.Z.; Jiang, L.L.; Wang, X.Y. The effect of cations (NH₄⁺, Na⁺, K⁺, and Ca²⁺) on chemical deactivation of commercial SCR catalyst by bromides. *Chin. J. Catal.* **2018**, *39*, 710–717. [[CrossRef](#)]
39. Yin, X.; Han, H.; Gunji, I.; Endou, A.; Ammal, S.S.C.; Kubo, M.; Miyamoto, A. NH₃ adsorption on the brønsted and lewis acid sites of V₂O₅ (010): A periodic density functional study. *J. Phys. Chem. B* **1999**, *103*, 4701–4706. [[CrossRef](#)]
40. Ye, J.; Gao, X.; Zhang, Y.; Wu, W.; Song, H.; Luo, Z.; Cen, K. Effects of PbCl₂ on selective catalytic reduction of NO with NH₃ over vanadia-based catalysts. *J. Hazard. Mater.* **2014**, *274*, 270–278.
41. Yang, Y.; Xu, W.; Wu, Y.; Wang, J.; Zhu, T. Inhibition effect of HBr over a commercial V₂O₅-WO₃/TiO₂ catalyst in a NH₃-SCR process. *Catal. Commun.* **2017**, *94*, 82–85. [[CrossRef](#)]
42. Yang, J.; Yang, Q.; Sun, J.; Liu, Q.; Zhao, D.; Gao, W.; Liu, L. Effects of mercury oxidation on V₂O₅-WO₃/TiO₂ catalyst properties in NH₃-SCR process. *Catal. Commun.* **2015**, *59*, 78–82. [[CrossRef](#)]
43. Sheng, H.; Zhou, J.; Zhu, Y.; Luo, Z.; Ni, M.; Cen, K. Mercury oxidation over a Vanadia-based selective catalytic reduction catalyst. *Energy Fuels* **2009**, *23*, 253–259.
44. Sudarsan, V.; Muthe, K.P.; Vyas, J.C.; Kulshreshtha, S.K. PO₄³⁻ tetrahedra in SbPO₄ and SbOPO₄: A ³¹P NMR and XPS study. *J. Alloys Compd.* **2002**, *336*, 119–123. [[CrossRef](#)]
45. Jiang, H.; Wang, Q.; Zang, S.; Li, J.; Wang, Q. Enhanced photoactivity of Sm, N, P-tridoped anatase-TiO₂ nano-photocatalyst for 4-chlorophenol degradation under sunlight irradiation. *J. Hazard. Mater.* **2013**, *261*, 44–54. [[CrossRef](#)] [[PubMed](#)]
46. Lei, T.; Li, Q.; Chen, S.; Liu, Z.; Liu, Q. KCl-induced deactivation of V₂O₅-WO₃/TiO₂ catalyst during selective catalytic reduction of NO by NH₃: Comparison of poisoning methods. *Chem. Eng. J.* **2016**, *296*, 1–10. [[CrossRef](#)]
47. Zhang, S.; Li, H.; Zhong, Q. Promotional effect of F-doped V₂O₅-WO₃/TiO₂ catalyst for NH₃-SCR of NO at low-temperature. *Appl. Catal. A Gen.* **2012**, *435–436*, 156–162. [[CrossRef](#)]
48. Li, Q.; Chen, S.; Liu, Z.; Liu, Q. Combined effect of KCl and SO₂ on the selective catalytic reduction of NO by NH₃ over V₂O₅/TiO₂ catalyst. *Appl. Catal. B Environ.* **2015**, *164*, 475–482. [[CrossRef](#)]
49. You, Y.; Shi, C.; Chang, H.; Guo, L.; Xu, L.; Li, J. The promoting effects of amorphous CePO₄ species on phosphorus-doped CeO₂/TiO₂ catalysts for selective catalytic reduction of NO_x by NH₃. *Mol. Catal.* **2018**, *453*, 47–54. [[CrossRef](#)]
50. van Der Bij, H.E.; Weckhuysen, B.M. Phosphorus promotion and poisoning in zeolite-based materials: Synthesis, characterisation and catalysis. *Chem. Soc. Rev.* **2015**, *44*, 7406–7428. [[CrossRef](#)]
51. Yang, S.; Wang, C.; Ma, L.; Peng, Y.; Qu, Z.; Yan, N.; Chen, J.; Chang, H.; Li, J. Substitution of WO₃ in V₂O₅/WO₃-TiO₂ by Fe₂O₃ for selective catalytic reduction of NO with NH₃. *Catal. Sci. Technol.* **2013**, *3*, 161–168. [[CrossRef](#)]
52. Szalenić, M.; Drzewiecka-Matuszek, A.; Witko, M.; Hejduk, P. Ammonium adsorption on Brønsted acidic centers on low-index vanadium pentoxide surfaces. *J. Mol. Model.* **2013**, *19*, 4487–4501. [[CrossRef](#)] [[PubMed](#)]
53. Shen, B.; Wang, F.; Zhao, B.; Li, Y.; Wang, Y. The behaviors of V₂O₅-WO₃/TiO₂ loaded on ceramic surfaces for NH₃-SCR. *J. Ind. Eng. Chem.* **2016**, *33*, 262–269. [[CrossRef](#)]

